

# Formulation, optimization, and pharmacodynamic evaluation of chitosan/phospholipid/ $\beta$ -cyclodextrin microspheres

Lu Shan<sup>1</sup>  
En-Xue Tao<sup>2</sup>  
Qing-Hui Meng<sup>3</sup>  
Wen-Xia Hou<sup>3</sup>  
Kang Liu<sup>1</sup>  
Hong-Cai Shang<sup>4</sup>  
Jin-Bao Tang<sup>1</sup>  
Wei-Fen Zhang<sup>1,4</sup>

<sup>1</sup>School of Pharmacy, Weifang Medical University, <sup>2</sup>The Affiliated Hospital of Weifang Medical University, <sup>3</sup>School of Nursing, Weifang Medical University, Weifang, <sup>4</sup>Key Laboratory of Chinese Internal Medicine of Ministry of Education and Beijing, Dongzhimen Hospital, Beijing University of Chinese Medicine, Beijing, People's Republic of China

**Abstract:** Cholinergic neurotransmission loss is the main cause of cognitive impairment in patients with Alzheimer's disease. Phospholipids (PLs) play an essential role in memory and learning abilities. Moreover, PLs act as a source of choline in acetylcholine synthesis. This study aimed to prepare and optimize the formulation of chitosan/phospholipid/ $\beta$ -cyclodextrin (CTS/PL/ $\beta$ -CD) microspheres that can improve cognitive impairment. The CTS/PL/ $\beta$ -CD microspheres were prepared by spray drying, and optimized with an orthogonal design. These microspheres were also characterized in terms of morphology, structure, thermostability, drug loading, and encapsulation efficiency. The spatial learning and memory of rats were evaluated using the Morris water maze test, and the neuroprotective effects of the CTS/PL/ $\beta$ -CD microspheres were investigated by immunohistochemistry. Scanning electron microscopic images showed that the CTS/PL/ $\beta$ -CD microspheres were spherical with slightly wrinkled surfaces. Fourier transform infrared spectroscopy and differential scanning calorimetry proved that PLs formed hydrogen bonds with the amide group of CTS and the hydroxyl group of  $\beta$ -CD. The learning and memory abilities of rats in the treated group significantly improved compared with those in the model group. Immunohistochemical analysis revealed that treatment with the CTS/PL/ $\beta$ -CD microspheres attenuated the expression of protein kinase C- $\delta$  and inhibited the activation of microglia. These results suggest that the optimized microspheres have the potential to be used in the treatment of Alzheimer's disease.

**Keywords:** chitosan, spray drying, microsphere, Alzheimer's disease, phospholipids

## Introduction

Alzheimer's disease (AD) is a progressive neurodegenerative disorder in which the death of brain cells causes memory loss and cognitive decline, consequently affecting the quality of life of the patients. Despite substantial works, the pathological mechanism of AD remains incompletely understood. Recently, accumulating evidence suggested the significance of the extracellular deposition of amyloid beta (A $\beta$ ) peptide in senile plaques; this proposition is known as the "amyloid cascade hypothesis".<sup>1-4</sup> To ameliorate cognitive deficit and memory dysfunction, most patients with AD are administered acetylcholinesterase inhibitors, which can enhance cholinergic neurotransmission. However, these agents provide unsatisfactory results because of low bioavailability and undesirable side effects.

Phospholipids (PLs) are important components of cell membranes and act as precursors of acetylcholine; therefore, PLs can be adopted as a main source of choline to improve learning and memory abilities.  $\beta$ -Cyclodextrin ( $\beta$ -CD) is a natural cyclic oligosaccharide with a lipophilic central cavity and a hydrophilic outer surface.<sup>5</sup> Similar to other CDs,  $\beta$ -CD is characterized by its capacities to improve drug stability,

Correspondence: Jin-Bao Tang;  
Wei-Fen Zhang  
School of Pharmacy, Weifang Medical University, 7166 Baotong West Street, Weifang, Shandong 261053, People's Republic of China  
Tel +86 536 846 2490  
Fax +86 536 878 5609  
Email tangjb@wfmcc.edu.cn;  
zhangwf@wfmcc.edu.cn

increase drug absorption and solubility, control drug release, and mask unpleasant smell;<sup>6</sup> these properties contribute to the wide application of  $\beta$ -CD in the pharmaceutical field. Chitosan (CTS), a natural cationic polysaccharide composed of glucosamine and *N*-acetylglucosamine by  $\beta$ -(1, 4)-linkage, is well known for its excellent biocompatibility and biodegradability, as well as low toxicity.<sup>7,8</sup> At present, CTS is used as a promising drug carrier in various pharmaceutical formulations, particularly nanodrug delivery systems.<sup>9</sup> With regard to its strong antioxidant activity, CTS can not only inhibit A $\beta$  formation but can also effectively suppress oxidative stress-induced neurotoxicity,<sup>10–12</sup> indicating its potential use as a neuroprotective agent. According to our previous study, PLs and CTS can accelerate each other's absorption rate when used in combination, resulting in a sustained therapeutic effect.<sup>13</sup>

The present study was designed to prepare a microsphere delivery system consisting of CTS, PL, and  $\beta$ -CD for AD treatment. First, CTS/PL/ $\beta$ -CD microspheres were prepared by a spray-drying method, and their formulation was optimized with an orthogonal design. The pharmaceutical properties of the microspheres were evaluated on the basis of their morphological information, size, drug-loading capacities, encapsulation efficiency, moisture uptake, water content, and tap density. Their therapeutic effects were then assessed in AD model rats through Morris water maze test, and the possible underlying mechanism was also discussed.

## Materials and methods

### Materials

CTS (with a degree of deacetylation of 85%) was purchased from Haili Biological Products Co., Ltd. (Laizhou, Shandong, People's Republic of China). Glacial acetic acid was bought from Qingdao Haibin Reagent Company (Qingdao, People's Republic of China). PLs were supplied by Shanghai Advanced Vehicle Technology Pharmaceutical Co., Ltd. (Shanghai, People's Republic of China).  $\beta$ -CD was obtained from Chengdu Kelong Chemical Reagent Factory (Chengdu, People's Republic of China). Sodium dihydrogen phosphate and disodium hydrogen phosphate were provided by Shanghai Chemical Reagent Company (Shanghai, People's Republic of China). Other chemicals used were of analytical grade.

### Preparation and optimization of CTS/PL/ $\beta$ -CD microspheres

Predetermined amounts of PLs and  $\beta$ -CD, which were dried in vacuo at room temperature, were dissolved in 200 mL of

1% CTS in acetic acid aqueous solution followed by filtration (0.45  $\mu$ m syringe filters). Filtrates were subjected to a spray-drying process by using a spray dryer with two-fluid nozzles (Mini Spray-Dryer, B-290; Büchi Labortechnik AG, Flawil, Switzerland). The optimum parameters for the formulation of CTS/PL/ $\beta$ -CD microspheres were determined using an  $L_9(3^4)$  orthogonal design with three levels of the four following factors: inlet temperature, feeding rate, air flow rate, and CTS/PL/ $\beta$ -CD ratio (Table 1). Blank microspheres were prepared using the same procedures for controls. The resultant microspheres were collected and stored in a desiccator over anhydrous calcium chloride at room temperature before use.

### Characterization of CTS/PL/ $\beta$ -CD microspheres

The microspheres prepared at various CTS/PL/ $\beta$ -CD ratios were sputtered with a thin layer of gold/palladium alloy prior to morphological measurement by scanning electron microscopy (s4500n; Hitachi High-tech Science Corporation, Tokyo, Japan). Their infrared absorption spectra were determined by Fourier transform infrared spectroscopy (Avatar-360; Shanghai Lengguang Technology Co., Ltd. Shanghai, People's Republic of China). The scanning process was conducted in the wavenumber range of 400–4,000  $\text{cm}^{-1}$ . Changes in the thermal property of the microspheres were measured by differential scanning calorimetry (DSC) using DSC7020 (Beijing Saisimeng Instrument Co., Ltd., Beijing, People's Republic of China).

### Determination of drug loading and encapsulation efficiency

An equivalent of microspheres (100 mg) was first dissolved in 10 mL of 0.5 mol/L acetic acid solution, which was then transferred to a volumetric flask and diluted with distilled water to a final volume of 1.0 L. Afterward, 1 mL of filtrate was added to a 10 mL volumetric flask and diluted to a volume of 10 mL with distilled water. The absorbance of the resultant solution was measured at 605 nm and was then applied to calculate the concentration of CTS by using the following equation:  $A=0.0593C+0.1459$  ( $n=6$ ;  $r=0.9999$ ).

**Table 1** The factors and levels discussed in the orthogonal design

Levels	Factors			
	$T_{\text{inlet}}$ ( $^{\circ}\text{C}$ )	Feeding rate (mL/min)	Air flow rate (L/h)	CTS/PL/ $\beta$ -CD ratio
1	190	12	700	1:1:0.33
2	170	8	400	2:1:0.33
3	150	14	300	3:1:0.67

**Abbreviations:**  $T_{\text{inlet}}$ , inlet temperature; CTS, chitosan; PL, phospholipid;  $\beta$ -CD,  $\beta$ -cyclodextrin.

The amount of loaded drug in the microspheres was determined by UV spectrophotometry (UV-Vis with UV-8000A Spectrophotometer; Shanghai Puxi Instrument Factory, Shanghai, People's Republic of China). Drug loading (DL) and encapsulation efficiency (EE) were calculated using the following equations:

$$DL(\%) = \frac{\text{Actual drug content}}{\text{Weight of the microspheres}} \times 100 \quad (1)$$

$$EE(\%) = \frac{\text{Actual drug content}}{\text{Theoretical drug content}} \times 100 \quad (2)$$

All tests were performed in triplicate and average values were plotted.

### Tap density

The tap density of the microspheres was determined in accordance with the United States Pharmacopoeia appendix method. Briefly, the microspheres were loaded in a 5 mL test tube before being tapped from a predetermined height (14 mm) on a hard bench top. Mechanical tapping was measured as prescribed (20 times). The test tube was loaded with microspheres until a constant volume was achieved. The microspheres were then weighed while the bulk of the test tube was measured. The Carr's index was calculated using the following equation:

$$\text{Carr's index}(\%) = \frac{\text{Tapped density} - \text{Bulk density}}{\text{Tapped density}} \times 100 \quad (3)$$

### Swelling behavior

The swelling behavior of the microspheres was assessed by measuring the water uptake. Briefly, dried microspheres were weighed ( $W_d$ ) before being dispersed in a 5 mL test tube containing 4 mL of phosphate-buffered saline (pH 6.8). After thorough mixing by vortex for 5 minutes, the resultant mixture was incubated with phosphate-buffered saline at pH 6.8 for 12 hours to achieve swelling equilibrium. Subsequently, the solution was centrifuged and the water on the surface of microspheres was removed with filter paper and weighed immediately on an electronic balance. The weight of swollen microspheres ( $W_w$ ) was recorded. The swelling ratio was determined using the following equation:

$$\text{Swelling ratio}(\%) = \frac{W_w - W_d}{W_w} \times 100 \quad (4)$$

All experiments were performed in triplicate.

### Determination of moisture uptake

Briefly, 100 mg of the microspheres ( $W_d$ ) was dried to constant weight under vacuum and then filled into polystyrene tubes. These tubes were placed in a chamber at 40°C/relative humidity (RH) 75%. The weight of the microspheres ( $W_h$ ) was recorded at the end of different predetermined intervals (0.5, 1, 2, 4, 8, 12, and 24 hours), in which any increase in weight indicated the amount of moisture uptake. The weight ratio of the absorbed moisture was calculated at each time period as follows:

$$\text{Weight ratio}(\%) = \frac{W_h - W_d}{W_h} \times 100 \quad (5)$$

Each sample was analyzed thrice.

### Moisture content

The moisture content of the microspheres was estimated through thermogravimetric analysis. Briefly, an appropriate amount of microspheres were placed in a weighing bottle, which was heated from 25°C to 105°C for 4 hours followed by equilibration at 105°C for another 0.5 hour. The microspheres were stored in closed containers at room temperature. Thermogravimetric analysis was performed shortly after spray drying, and the weight loss after drying indicated moisture content.

### Animals

Female Wistar rats weighting 260–340 g were obtained from Shandong Lukang Pharmaceutical Co. Ltd (Shandong, People's Republic of China). The animals were maintained in a temperature- and humidity-controlled environment with a 12:12 hour light–dark cycle. Feed and water were available ad libitum. All experimental procedures were conducted in accordance with the US NIH Guidelines for the Care and Use of Laboratory Animals, and the animal study was approved by the animal ethical committee of Weifang Medical University.

### In vivo AD model

A total of 40 rats, which were fasted for 24 hours, were first anesthetized with 10% chloral hydrate before slowly injecting them with 5 mg/mL  $A\beta_{25-35}$  in sterile distilled water (incubated at 37°C for 7 days before use) into the hippocampus by using the following stereotaxic coordinates: 3.5 mm posterior to the bregma, 2.5 mm lateral to the midline, and 3.0 mm ventral to the skull surface. Syringe needles were kept in place for 6 minutes before gentle withdrawal. Meanwhile, 10 normal rats were subjected to sham operation.

## Experimental procedures

The model rats were randomly divided into four groups (n=10) according to their corresponding oral administration with normal saline (model group) or 20, 60, or 100 mg/kg/day of CTS/PL/ $\beta$ -CD microspheres in normal saline (low, medium, or high group, respectively) once per day for 30 days. Meanwhile, sham-operated rats were injected with the same volume of normal saline.

## Morris water maze test

The Morris water maze was adopted to determine the effects of CTS/PL/ $\beta$ -CD microspheres on the spatial memory and learning of AD model rats, as described previously.<sup>14–16</sup> The experimental facilities consisted of a circular water pool and an escape platform located below the water surface and at the center of the southwest quadrant. The indicators of behavior assessment consisted of navigation testing and probe trial. Rats were prehandled within 2 weeks before the Morris water maze test. The rats received four trials daily for 5 days consecutively. Each trial lasted for 120 seconds. At the beginning of each trial, the rats were placed into the water with their noses pointing to the tank wall. Each rat was allowed to swim freely for 120 seconds to seek the platform. If the rats found the platform within 120 seconds, they were allowed to rest on the platform for 5 seconds, and their escape latency was recorded. If the rats failed to reach the platform, they were guided to it and allowed to remain there for 5 seconds, and the score was 120 seconds. The average escape latency was determined for subsequent analysis. The probe trial was conducted on the sixth day when the extent of memory consolidation was assessed. In the probe trial, the platform was removed, and the rats were placed in the northeast quadrant and allowed to swim freely for 120 seconds. The rats received two trials per day. The numbers of crossings over the position at which the platform had been located were recorded as indexes of spatial memory. The results of daily trials were averaged for each rat. All behavioral data were recorded using a computerized video tracking system.

## Immunohistochemical staining

After treatment, the rats were deeply anesthetized with 10% chloral hydrate before perfusion through the heart with normal saline until the liver turned pale. The heart was further perfused with 4% paraformaldehyde until the limb and tail became stiff. The brain was then isolated and fixed in 4% paraformaldehyde for 24 hours before being embedded in paraffin for histological analysis. The obtained paraffin sections (3  $\mu$ m) were dewaxed and brought to water through graded ethanol. The sections were then incubated with

0.3% H<sub>2</sub>O<sub>2</sub> at room temperature for 20 minutes to quench endogenous peroxidase activity. Incubation with primary antibodies against protein kinase C- $\delta$  (PKC- $\delta$ ) and ionized calcium-binding adaptor molecule-1 (Iba1) (diluted 1:10) was conducted at 4°C overnight. After washing, the sections were sequentially exposed to secondary antibodies (universal IgG antibody–Fab segment–horse-radish peroxidase multimeric) at 37°C for 30 minutes. The resultant sections were stained with 3,3'-diaminobenzidine at room temperature, placed in hematoxylin, and then mounted with neutral resin. Images were observed and captured with the Leica DM1000 automated upright microscope system.

## Statistical analysis

All data in different experiments are shown as mean  $\pm$  standard deviation (SD). Differences between the groups were assessed by one-way analysis of variance (ANOVA). Significant differences were represented as  $P < 0.05$ .

## Results and discussion

### Orthogonal design for the optimization of experimental conditions

DL and EE are important indexes to assess the quality of microspheres. To optimize the formulation, an L<sub>9</sub>(3<sup>4</sup>) orthogonal design was established in which four factors, namely, inlet temperature, feeding rate, air flow rate, and CTS:PL: $\beta$ -CD ratio (labeled as A, B, C, and D in Table 2), were investigated at three levels. The microspheres produced DL ranging from 0.21% to 5.08% and EE from 0.50% to 9.53%. The DL and EE values increased with the increase in drug-to-carrier ratio. As shown in Table 2, the optimal formulation was drawn as follows: 150°C inlet temperature, feeding rate of 8 mL/min, air flow rate of 300 L/h, and CTS/PL/ $\beta$ -CD ratio of 1:1:0.33.

**Table 2** Results of the orthogonal design

Run number	A (°C)	B (mL/min)	C (L/h)	D	DL (%)	EE (%)
1	190	12	700	1/1/0.33	3.07 $\pm$ 0.13	7.15 $\pm$ 0.46
2	190	8	400	2/1/0.33	2.70 $\pm$ 1.78	3.39 $\pm$ 1.13
3	190	14	300	3/1/0.67	2.44 $\pm$ 1.31	3.77 $\pm$ 1.23
4	170	12	400	3/1/0.67	0.21 $\pm$ 0.04	0.50 $\pm$ 0.13
5	170	8	300	1/1/0.33	3.14 $\pm$ 2.31	5.01 $\pm$ 1.45
6	170	14	700	2/1/0.33	0.42 $\pm$ 0.12	0.71 $\pm$ 0.22
7	150	12	300	2/1/0.33	4.93 $\pm$ 0.16	8.71 $\pm$ 0.23
8	150	8	700	3/1/0.67	4.03 $\pm$ 0.57	7.78 $\pm$ 0.32
9	150	14	400	1/1/0.33	5.08 $\pm$ 0.15	9.53 $\pm$ 0.69

**Notes:** A, inlet temperature; B, feeding rate; C, air flow rate; and D, CTS/PL/ $\beta$ -CD ratio. Data in the "DL" and "EE" columns presented as mean  $\pm$  standard deviation.

**Abbreviations:** CTS, chitosan; PL, phospholipid;  $\beta$ -CD,  $\beta$ -cyclodextrin; DL, drug loading; EE, encapsulation efficiency.

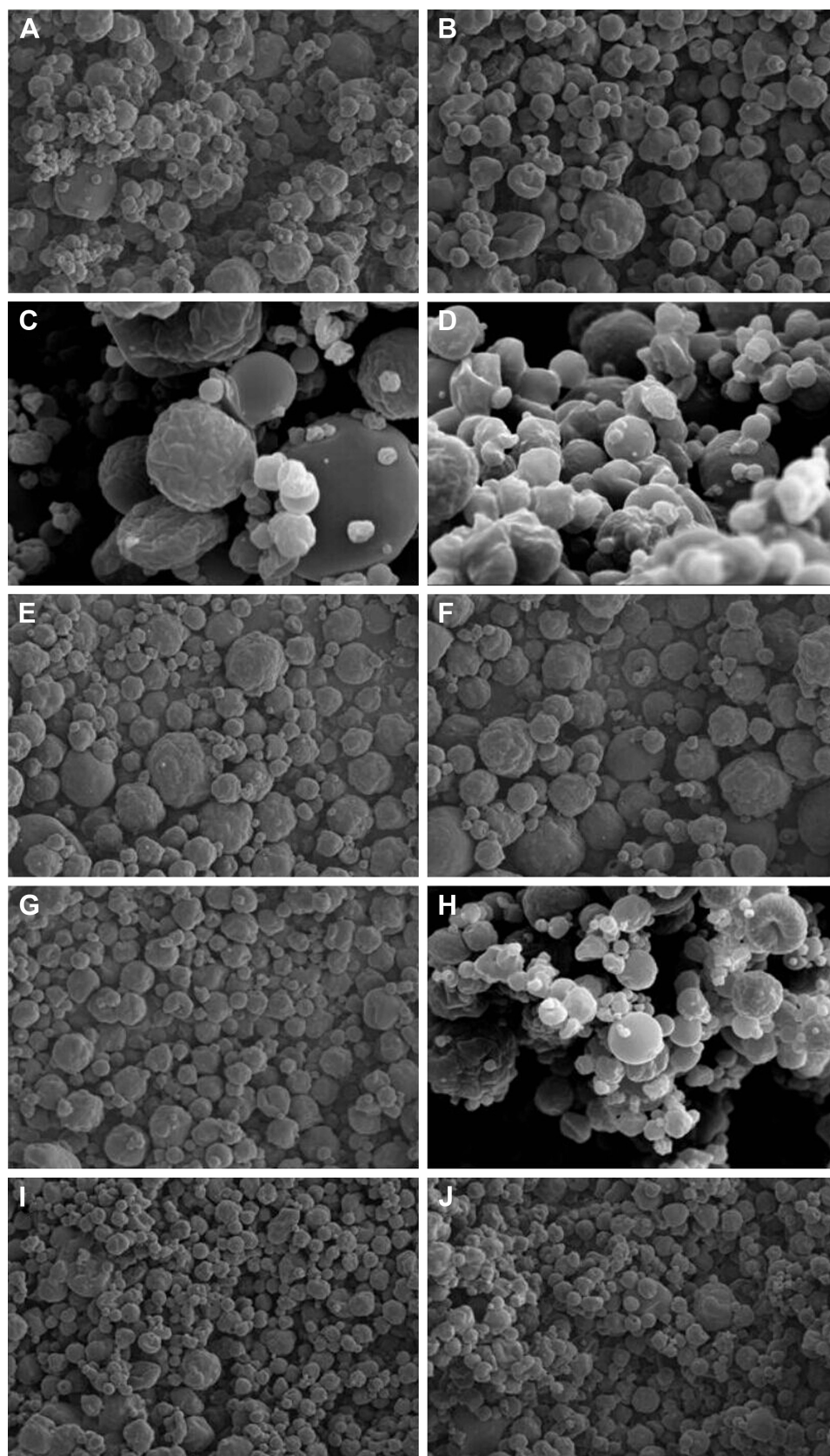


**Figure 1** The SEM of spray-drying microspheres.

**Notes:** The magnification is 3,000 $\times$ . (A) 190°C, 12 mL/min, 700 L/h, 1:1:0.33; (B) 190°C, 8 mL/min, 400 L/h, 2:1:0.33; (C) 190°C, 14 mL/min, 300 L/h, 3:1:0.67; (D) 170°C, 12 mL/min, 400 L/h, 3:1:0.67; (E) 170°C, 8 mL/min, 300 L/h, 1:1:0.33 (F) 170°C, 14 mL/min, 700 L/h, 2:1:0.33; (G) 150°C, 12 mL/min, 300 L/h, 2:1:0.33; (H) 150°C, 8 mL/min, 700 L/h, 3:1:0.67; (I) 150°C, 14 mL/min, 400 L/h, 1:1:0.33; and (J) 150°C, 8 mL/min, 300 L/h, 1:1:0.33.

**Abbreviation:** SEM, scanning electron microscope.

## Characteristics of the microspheres

### Particle size and morphology

CTS/PL/ $\beta$ -CD microspheres were produced using pre-determined parameters in the spray-drying process, and their morphological information was estimated by scanning electron microscopy. After spray drying at a ratio of 3:1:0.67, the obtained micrographs indicated a broader size distribution (Figure 1). A larger particle size can be obtained by decreasing the compressed air flow, increasing the feed rate, or raising the nozzle diameter.<sup>17</sup> In this study, the increase in particle size may be attributed to the difference in the rate of feeding. Nebulization of feeds at a higher rate may result in the formation of larger particles.<sup>18</sup> Furthermore, microspheres A, B, E, F, G, and I (Figure 1) showed a regular spherical shape and adhesion phenomenon, indicating their unsatisfactory fluidity. Some crystals were also found on the surface of these microspheres because CTS or PL was unsuccessfully entrapped within them. Similar to previous reports,<sup>19</sup> wrinkled surfaces were observed on the microspheres, which may have resulted from excessive vapor pressure in the spray-drying process.<sup>20</sup> Under the same conditions, smaller, well-distributed microspheres were prepared using a nozzle orifice diameter of 1.4 mm instead of 0.7 mm. Microsphere J was prepared using the optimal

formulation and it presented a uniform spherical shape and slightly wrinkled surfaces (Figure 1). The wrinkled particles exhibited a higher area for specific surface and were easier to disperse.<sup>21</sup>

### Fourier transform infrared spectroscopy

The Fourier transform infrared spectra of CTS, PL, CTS/PL, and CTS/PL/ $\beta$ -CD microspheres are shown in Figure 2. The strong peaks at 1,735 and 1,156  $\text{cm}^{-1}$  in PLs were attributed to C=O and P=O stretches, respectively. The strong peaks at 2,905 and 2,996  $\text{cm}^{-1}$  and the weak peaks at 1,400  $\text{cm}^{-1}$  in PLs resulted from the stretching and deformation of methyl groups. No significant differences were found among the spectra of CTS (Figure 2A), PL (Figure 2B), and CTS/PL microspheres (Figure 2C); briefly, no interaction existed between CTS and PL. In CTS/PL/ $\beta$ -CD microspheres (Figure 2D), strong bands at 3,000  $\text{cm}^{-1}$  were observed, indicating the formation of intermolecular hydrogen bonds between CTS (N–H stretch) and  $\beta$ -CD (O–H stretch). The peak at 3,400  $\text{cm}^{-1}$  was remarkably strengthened, which showed an overlap between  $\beta$ -CD (O–H stretch) and CTS (O–H stretch, N–H stretch) after spray drying. The peaks at 1,300 to 900  $\text{cm}^{-1}$  were markedly enhanced because of the increase in the stretching vibration of C–H, C–O, and P–O single bonds and C=O, P=O double bonds.<sup>22</sup>

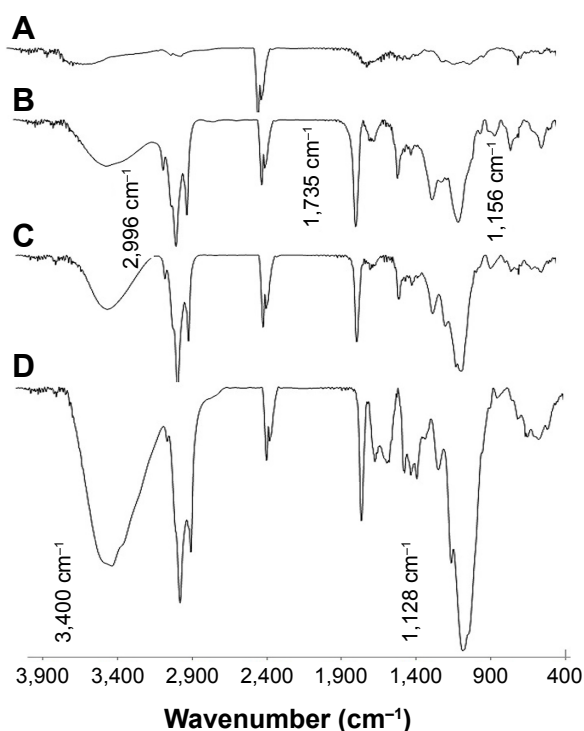


**Figure 2** The FTIR spectra of (A) CTS, (B) PL, (C) CTS/PL MS, and (D) CTS/PL/ $\beta$ -CD MS. **Abbreviations:** FTIR, Fourier transform infrared; CTS, chitosan; PL, phospholipid; MS, microspheres;  $\beta$ -CD,  $\beta$ -cyclodextrin.

### Differential scanning calorimetry

DSC provides precise and accurate quantitative data because of separate treatment of the sample and the reference based on the power-compensated “null balance” principle.<sup>23</sup> The DSC thermograms of CTS/PL/ $\beta$ -CD microspheres, CTS alone, PL alone, and PL/ $\beta$ -CD mixture are shown in Figure 3. The presence of several smaller peaks under 100°C indicated that the samples were not dry. The thermogram of CTS showed a weak peak at 288.94°C and a strong peak at 502.78°C, which represented the side-chain and backbone endothermic peaks, respectively. By contrast, the thermogram of PL displayed double peaks at 368.87°C and 394.38°C, which represented the side-chain and backbone endothermic peaks at 517.60°C. In the thermogram of PL/ $\beta$ -CD, endothermic peaks were produced at 373.61°C and 374.66°C for the side chain and at 511.26°C for the backbone. Furthermore, the thermogram of CTS/PL/ $\beta$ -CD exhibited two endothermic peaks at 302.68°C and 343.37°C, as well as a single peak at 481.19°C, resulting in the splitting of melting endotherms of the side chain and backbone. These results demonstrated that the degradation temperature of CTS/PL/ $\beta$ -CD was lower than those of PL and PL/ $\beta$ -CD.

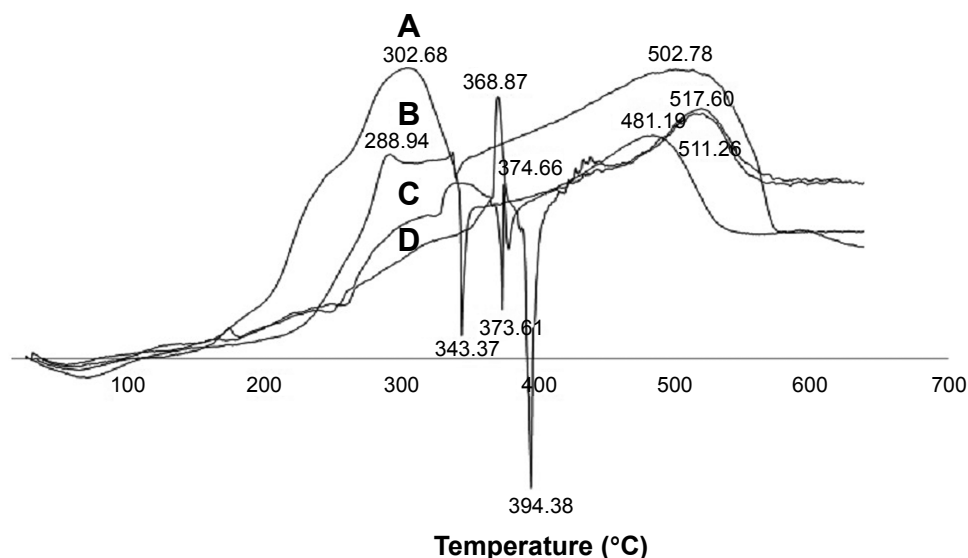


**Figure 3** The DSC thermograms of (A) CTS/PL/ $\beta$ -CD microspheres, (B) CTS, (C) PL, and (D) PL/ $\beta$ -CD mixture. **Abbreviations:** DSC, differential scanning calorimetry; CTS, chitosan; PL, phospholipid;  $\beta$ -CD,  $\beta$ -cyclodextrin.

### Moisture content

High moisture content may cause particle agglomeration, thereby decreasing the stability of the microspheres and their active components. Normally, the moisture content of particles should be  $<10\%$ .<sup>18</sup> In the present study, the moisture content of the microspheres ranged from 5.01% to 8.42%, which was low enough to assure the stability of the microspheres (Figure 4). Microspheres A and G presented large SD probably because the samples were placed in the inlet of the oven. The moisture contents of microspheres A, E, and I increased along with the increase of CTS concentrations, as well as microspheres B, F, G and C, D, H, indicating a possible relationship between moisture content and CTS. Low moisture content is highly desirable in microspheres, as it may hinder interparticle cohesion, avoid drug degradation, and attain long-term stability.<sup>24</sup> By contrast, high moisture content may negatively affect the stability of powders.<sup>25</sup>

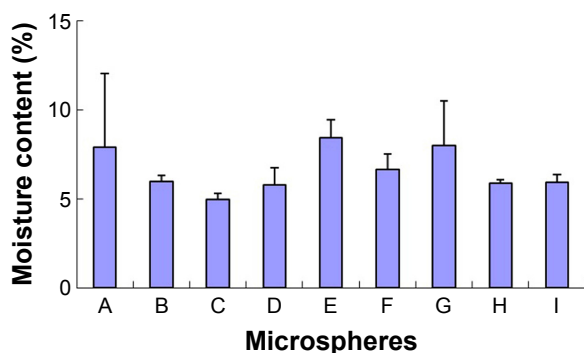


**Figure 4** The moisture content of microspheres under different fabrication conditions.

### Swelling behavior

Swelling behavior is essential to estimate the stability, adhesive capacities, release of loaded drugs, and cohesiveness of the microspheres. Bi et al<sup>26</sup> reported that low swelling behavior facilitates the stability of microspheres. As shown in Figure 5, the swelling rates of microspheres A, E, and I increased along with the increase of CTS concentrations, as well as microspheres B, F, G and C, D, H. However, no statistical differences in swelling behavior were observed, which may be explained by the various amounts of CTS used in the microspheres. By contrast, microspheres E, F, and H presented larger SD probably because the drug was swelled at different levels of dryness. In addition, drug powders were observed on filter sheets. The swelling behavior of microspheres can significantly influence the release of loaded drugs.<sup>20</sup> In the current study, loaded drugs were easier to release from the microspheres at a higher

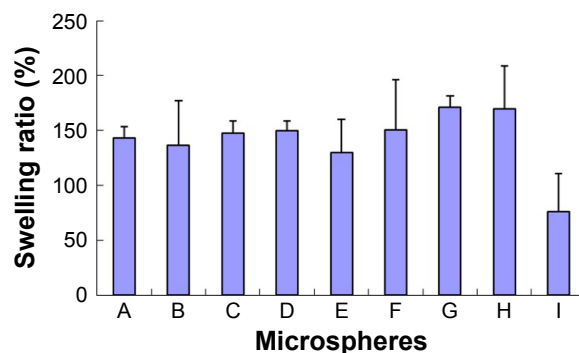


**Figure 5** The swelling ratio of microspheres under different fabrication conditions.

swelling rate. Therefore, the microspheres demonstrated good controlled-release capacity and can be applied as carriers for drug delivery.

### Tapped density

Tapped density is a significant physical property of microspheres, which provides important information about the true density, porosity of the particles, and particle-size distribution.<sup>27</sup> The Carr's index is considered to be an indirect index for the evaluation of powder flowability. Microspheres with >25% Carr's index are more likely to flow poorly. Typically, low bulk and tapped density indicate poor powder flowability.<sup>28</sup> In the current study, the tapped density of the microspheres ranged from 0.283 to 0.348 g/mL (Figure 6). The compressibility index of all the microspheres ranged from 12.9% to 24.9%, indicating good flow characteristics.<sup>27</sup> According to our previous study, the microspheres after spray drying are useful in a pulmonary drug delivery system, with satisfactory flowability and dispersibility.<sup>29</sup> These results indicate that the spray-drying conditions exerted no effect on tapped density, but this parameter increased along with the increase of the CTS ratio. The SD values of B and I were larger because of different knocking degrees to powder. Tapped density can be adopted as an indirect criterion to assess the abilities of microspheres to withstand the processing stresses of coating and drying; a denser material is more tolerant to stresses.<sup>30</sup>

### Moisture uptake

The duration of moisture uptake in the microspheres at 40°C/RH 75% is shown in Figure 7. The humidity rates of microspheres A–I within 0.5 hour were 3.98%–4.42%, 4.10%–4.48%, 5.27%–5.95%, 5.50%–6.06%, 3.53%–4.43%, 4.64%–5.92%, 3.67%–4.21%, 3.65%–4.59%, and 3.64%–4.14%, respectively. When the exposure time was extended, the humidity rates increased and achieved equilibrium within 6 hours. Thus, a slight increase in humidity was observed

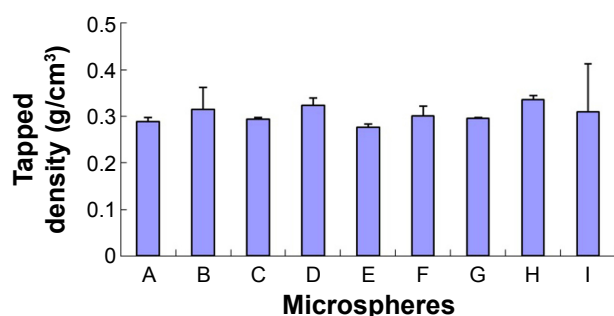


Figure 6 The tapped density of microspheres under different fabrication conditions.

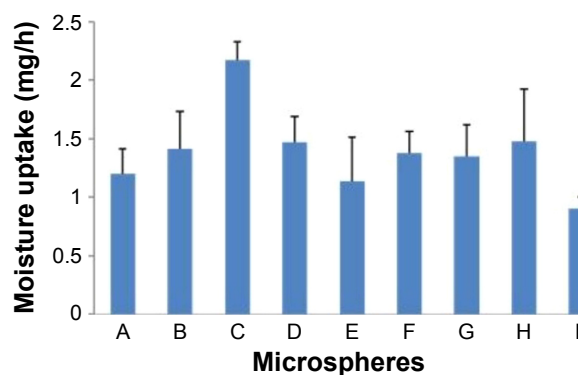


Figure 7 The moisture absorption rates of microspheres under different fabrication conditions.

when the microspheres were exposed at the same condition for 12 hours, namely 11.99%–12.21%, 11.95%–12.41%, 12.39%–13.03%, 12.60%–12.90%, 11.36%–11.74%, 11.99%–12.69%, 11.08%–11.76%, 12.11%–12.61%, and 10.98%–11.76%, respectively. In addition, the moisture uptake of the microspheres increased along with the increase of the CTS ratio (Figure 7). These results indicated that the microspheres can absorb moisture at 40°C/RH 75%. However, absorption may not occur if the microspheres are stored in inhalers. Considering that the humidity rate of the microspheres affects their stability and absorption in vivo, the microspheres should be kept from humid conditions during storage.

### Morris water maze acquisition

To determine whether CTS/PL/β-CD microspheres can attenuate AD-induced cognitive impairments, the learning and memory abilities of AD model rats were examined using the Morris water maze. Several studies have reported that Aβ<sub>25-35</sub> induced memory deficit in rat hippocampus, and it was used to successfully establish an AD model by Morris water maze.<sup>16,31,32</sup> In the present study, we selected rats to develop an AD model by injecting Aβ<sub>25-35</sub> in the hippocampus. As shown in Table 3, the mean time spent on day 1 in

Table 3 Effects of microspheres on escape latency in rats

Groups	Preoperative (t/s)	Postoperative 14 days (t/s)	Postoperative 30 days (t/s)
Control group	21.04±5.75	17.45±5.47	11.78±2.66 <sup>b</sup>
Model group	20.99±2.86	40.92±3.83 <sup>a</sup>	37.98±7.14
Low-dose group	20.13±6.97	38.73±2.48 <sup>a</sup>	17.82±1.66 <sup>b</sup>
Medium-dose group	21.70±8.32	37.47±2.89 <sup>a</sup>	16.86±3.12 <sup>b</sup>
High-dose group	22.21±3.92	36.94±2.94 <sup>a</sup>	15.75±1.59 <sup>b</sup>

Notes: <sup>a</sup>P<0.01 versus control group; <sup>b</sup>P<0.01 versus model group. Data (mean ± SD, n=10) obtained after the same treatment day are significantly different.

Abbreviations: SD, standard deviation; t/s, time/second.

escape latency was approximately 20 seconds in all groups, without any statistical intergroup differences. On day 14, an obvious increase was observed. A significant difference in escape latency ( $40.92 \pm 3.83$  vs  $17.45 \pm 5.47$  seconds;  $P < 0.01$ ) was shown between the model and control rats. These results demonstrated the successful establishment of the AD model rats through injection of  $A\beta_{25-35}$  in the hippocampus. As presented in Table 3, the escape latency ( $17.82 \pm 1.66$  seconds in the low-dose group,  $16.86 \pm 3.12$  seconds in the medium-dose group, and  $15.75 \pm 1.59$  seconds in the high-dose group vs  $37.98 \pm 7.14$  seconds in the model group;  $P < 0.01$ ) was remarkably different between the treatment and model groups. These results indicated that CTS/PL/ $\beta$ -CD microspheres can ameliorate the impairment of memory and learning abilities of rats induced by  $A\beta_{25-35}$ .

In the probe trial of the Morris water maze test, the rats in the model group swam around the entire pool and searched for the target platform without awareness. By contrast, the rats in the control and treatment groups swam in the target quadrant. The numbers of times crossing the platform position ( $1.1 \pm 0.21$  times vs  $4.80 \pm 0.63$  times;  $P < 0.01$ ) were significantly different between the model and control rats. On day 30, the rats in the model group swam aimlessly in the tank. As shown in Table 4, the numbers of times crossing the platform position ( $3.4 \pm 0.46$  times in the low-dose group,  $3.9 \pm 0.39$  times in the medium-dose group, and  $4.2 \pm 0.63$  times in the high-dose group vs  $1.3 \pm 0.48$  times in the model group;  $P < 0.01$ ) significantly differed between the treatment and model groups. These results indicated that injection of  $A\beta_{25-35}$  induced deficits in spatial memory, which can be alleviated by administration of CTS/PL/ $\beta$ -CD microspheres.

These results indicated that rats after  $A\beta_{25-35}$  injection showed behavioral changes, including reduced learning and memory. The learning and memory alterations in the Morris water maze test of the current study were consistent with previous reports,<sup>31–34</sup> which demonstrated that central

**Table 4** Effects of microspheres on the numbers of crossings over the former location of the platform by rats

Groups	Preoperative (time)	Postoperative 14 days (time)	Postoperative 30 days (time)
Control group	$4.10 \pm 0.66$	$4.80 \pm 0.63$	$4.65 \pm 0.58^b$
Model group	$4.20 \pm 0.54$	$1.10 \pm 0.21^a$	$1.30 \pm 0.48$
Low-dose group	$4.15 \pm 0.58$	$1.15 \pm 0.24^a$	$3.40 \pm 0.46^b$
Medium-dose group	$4.05 \pm 0.68$	$1.35 \pm 0.47^a$	$3.90 \pm 0.39^b$
High-dose group	$4.25 \pm 0.68$	$1.30 \pm 0.42^a$	$4.20 \pm 0.63^b$

**Notes:** <sup>a</sup> $P < 0.01$  versus control group; <sup>b</sup> $P < 0.01$  versus model group. Data (mean  $\pm$  SD,  $n = 10$ ) obtained after the same treatment day are significantly different.

**Abbreviation:** SD, standard deviation.

administration of  $\beta$ -amyloid peptides in rats can induce amnesia.  $A\beta_{25-35}$  aggregation is an important factor to neurotoxicity. Recent studies indicated that  $A\beta_{25-35}$  injection can markedly facilitate the onset of learning deficits.<sup>33</sup>

### Effect of CTS/PL/ $\beta$ -CD microspheres on the amounts of PKC- $\delta$ in the hippocampus

Recent reports showed that PKC- $\delta$  imbalance is important to cognitive impairment.<sup>35</sup> In the current study, AD model rats exhibited a considerable amount of immunoreactive cells in the cytoplasm (Figure 8E). However, fewer immunoreactive neurons were found in the cytoplasm of control rats (Figure 8A). Quantification analysis revealed significantly fewer immunoreactive neurons in the control group than in the model group ( $P < 0.05$ ; Table 5). Additionally, the number of immunoreactive neurons was remarkably higher in the model group than in the other groups (Figure 8B–E). Significantly fewer immunoreactive neurons were also detected in the treatment groups than in the model group ( $P < 0.05$ ). These results suggested that PKC- $\delta$  overexpression in the rat hippocampus led to NF- $\kappa$ B activation and caused an inflammatory response,<sup>36</sup> which are both essential to the etiology of AD. However, administration of CTS/PL/ $\beta$ -CD microspheres can prevent or weaken PKC- $\delta$  overexpression. In the present study,  $A\beta_{25-35}$  injection significantly increased the number of inflammatory cells in the hippocampus of AD rats, and PLs were found to reduce inflammation. However, this increase can be alleviated by CTS/PL/ $\beta$ -CD microspheres. The results were consistent with a report that PLs can effectively improve cognitive impairment. These results provided further evidence that CTS/PL/ $\beta$ -CD microspheres can exert a good therapeutic effect on AD by increasing doses.

### Effect of CTS/PL/ $\beta$ -CD microspheres on Iba1 expression in the hippocampus

In addition to PKC- $\delta$  overexpression, another key feature of AD neuropathology is microglia activation. Recently, researchers have demonstrated that  $A\beta_{25-35}$  can activate rat microglia, leading to neurodegeneration.<sup>37</sup> Microglia is an integral component of cored plaques in the brain with AD.<sup>38</sup> In the current study, microglial cells in the rats' brain sections were visualized immunohistochemically by using Iba1 antibody.<sup>39</sup> Hence, this study investigated the effects of CTS/PL/ $\beta$ -CD microspheres on  $A\beta_{25-35}$ -induced microglia activation. As shown in Table 5 and Figure 9, the majority of positive microglia exhibited a resting morphology in the saline-injected hippocampus (Figure 9A), whereas the model

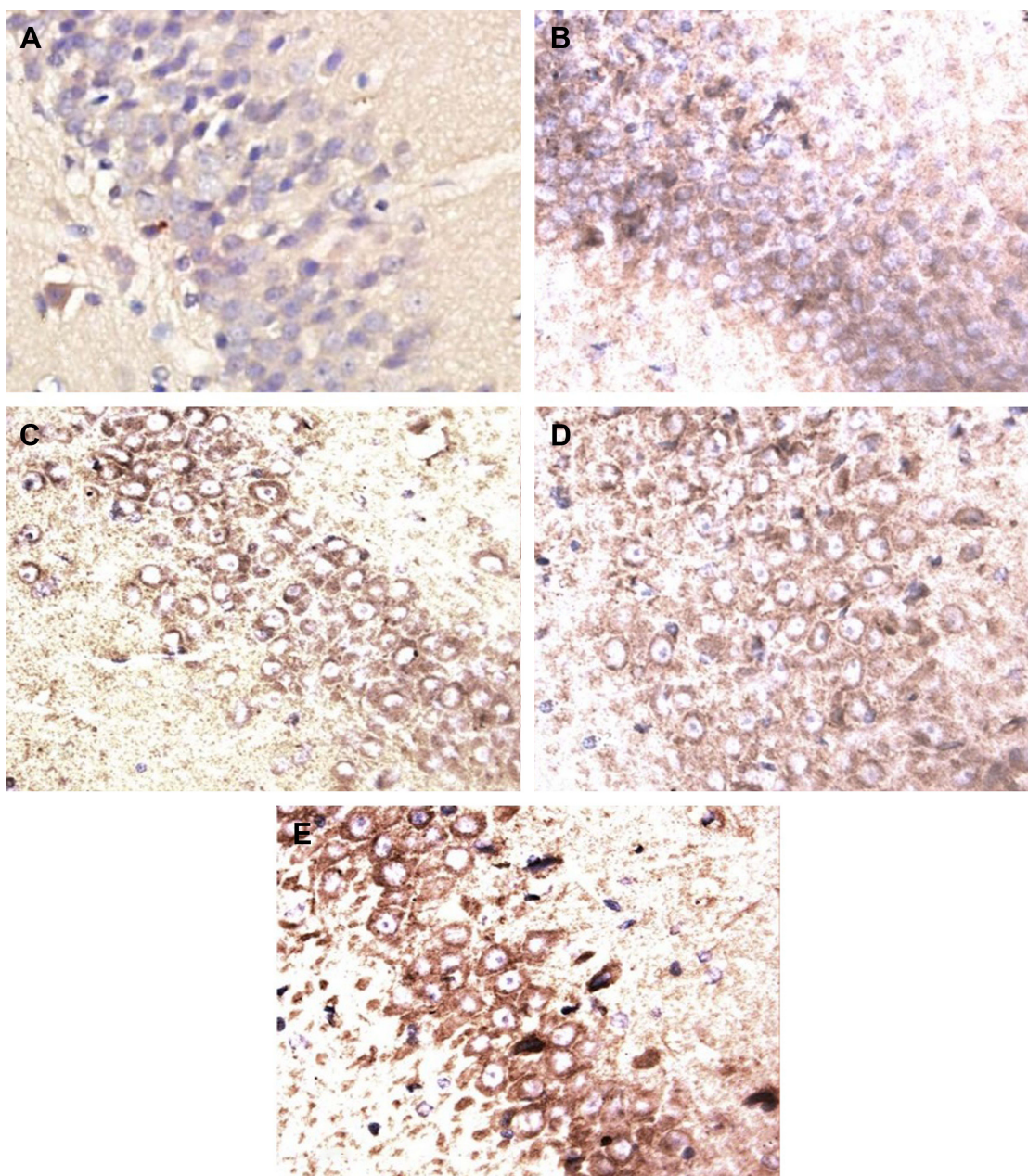


**Figure 8** Effects of CTS/PL/β-CD microspheres on the quantities of PKC-δ in the hippocampus by immunohistochemistry staining (light microscope, ×400).

**Notes:** (A) Control group, (B) high-dose group, (C) medium-dose group, (D) low-dose group, and (E) model group.

**Abbreviations:** CTS, chitosan; PL, phospholipid; β-CD, β-cyclodextrin; PKC-δ, protein kinase C-δ.

**Table 5** Effects of microspheres on the expression of PKC-δ and Iba1

Groups	PKC-δ	Iba1
Control group	15.0±3.68 <sup>a</sup>	16.2±3.32 <sup>b</sup>
High-dose group	25.9±3.17 <sup>a</sup>	33.0±5.20 <sup>b</sup>
Medium-dose group	30.9±3.69 <sup>a</sup>	39.4±4.25 <sup>b</sup>
Low-dose group	34.5±3.77 <sup>a</sup>	45.3±7.14 <sup>b</sup>
Model group	41.8±4.23	56.1±7.07

**Notes:** <sup>a</sup>*P*<0.05 versus model group; <sup>b</sup>*P*<0.05 versus model group. Data (mean ± SD, n=10) are obtained on the same day of treatment.

**Abbreviations:** SD, standard deviation; PKC-δ, protein kinase C-δ; Iba1, ionized calcium-binding adaptor molecule-1.

group showed activated microglia with large and thick cell bodies, as well as enhanced staining intensity processes (Figure 9E). Treatment with CTS/PL/β-CD microspheres gradually decreased the number of activated microglia compared with that in the model group (Figure 9B–D). These results indicated that CTS/PL/β-CD microspheres can inhibit the Aβ<sub>25-35</sub>-induced activation of microglia. Iba1 was detected in most cells, indicating microglia activation. CTS/PL/β-CD microspheres inhibited β-amyloid peptide deposition and microglial reaction. These findings

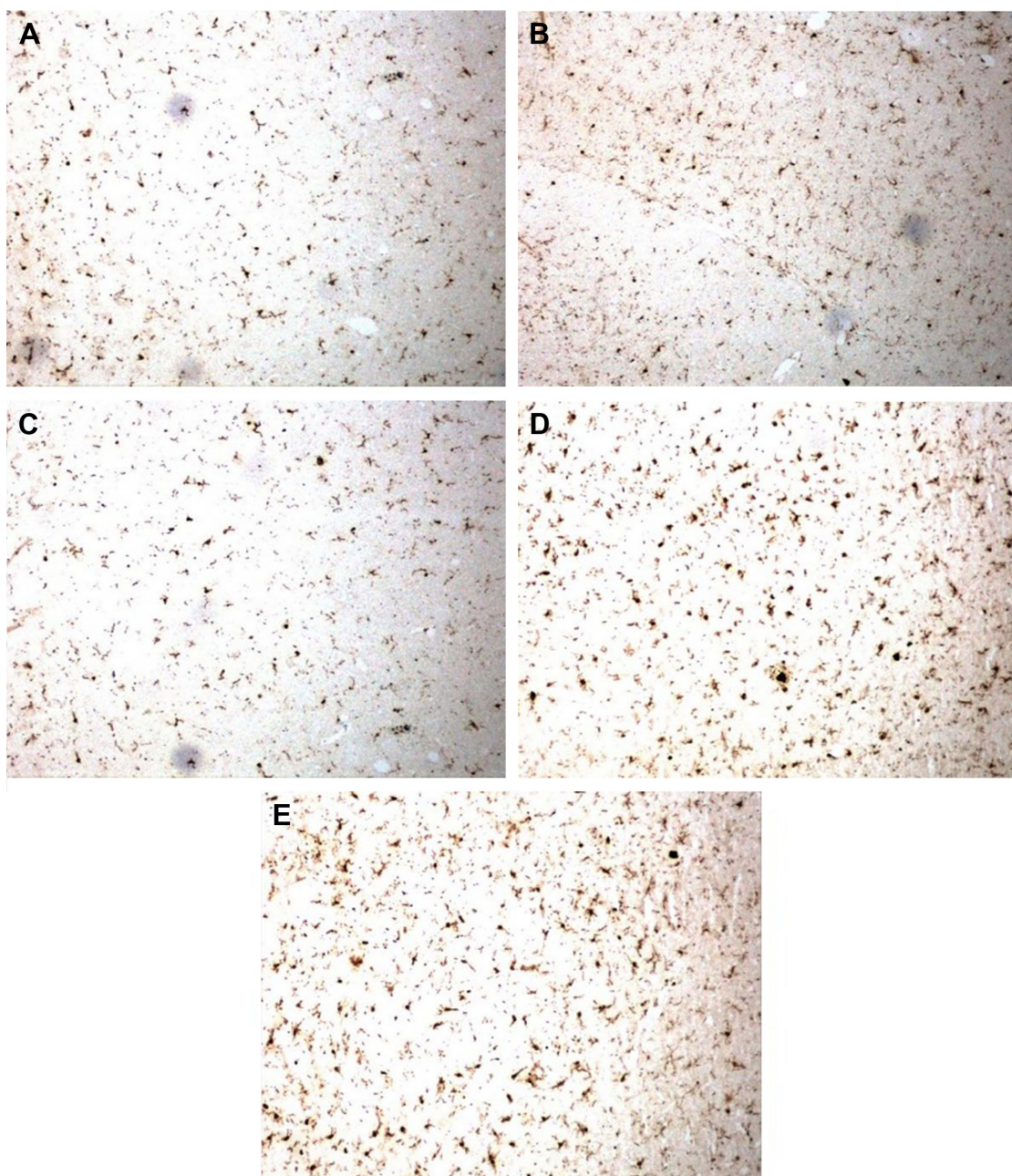


**Figure 9** Effects of CTS/PL/ $\beta$ -CD microspheres on the quantities of Iba1 in the hippocampus by immunohistochemistry staining (light microscope,  $\times 400$ ).

**Notes:** (A) Control group, (B) high-dose group, (C) medium-dose group, (D) low-dose group, and (E) model group.

**Abbreviations:** CTS, chitosan; PL, phospholipid;  $\beta$ -CD,  $\beta$ -cyclodextrin; Iba1, ionized calcium-binding adaptor molecule-1.

demonstrated that the microspheres suppress microglia activation; hence, the CTS/PL/ $\beta$ -CD microspheres are promising agents to treat AD.

## Conclusion

In this work, CTS/PL/ $\beta$ -CD microspheres were prepared by spray drying and optimized with an orthogonal design. The optimal formulation was established as follows: inlet temperature of  $150^{\circ}\text{C}$ , feeding rate of 8 mL/min, air flow rate

of 300 L/h, and CTS/PL/ $\beta$ -CD ratio of 1:1:0.33. Under the optimized conditions, the CTS/PL/ $\beta$ -CD microspheres exhibited positive characteristics such as uniform morphology and high specific surface area. Immunostaining analysis revealed that oral administration of CTS/PL/ $\beta$ -CD microspheres inhibited PKC- $\delta$  overexpression and microglia activation. In summary, this study established an optimum formulation for CTS/PL/ $\beta$ -CD microspheres, which are of potential value to treat AD.

## Acknowledgments

The authors gratefully acknowledge generous financial support from the National Key Technology Research and Development Program of the Ministry of Science and Technology, China (No 2013GA740103), National Natural Science Foundation of China (No 81573717), Natural Science Foundation of Shandong Province (ZR2012CM025, ZR2013HL066), and Department of Science and Technology of Weifang (2014WS045).

## Disclosure

The authors report no conflicts of interest in this work.

## References

- Kung HF. The  $\beta$ -amyloid hypothesis in Alzheimer's disease: seeing is believing. *ACS Med Chem Lett*. 2012;3(4):265–267.
- Naslund J, Haroutunian V, Mohs R, et al. Correlation between elevated levels of amyloid beta-peptide in the brain and cognitive decline. *JAMA*. 2000;283(12):1571–1577.
- Hardy J, Cullen K. Amyloid at the blood vessel wall. *Nat Med*. 2006;12(7):756–757.
- Selkoe DJ. The origins of Alzheimer's disease: a is for amyloid. *JAMA*. 2000;283(12):1615–1617.
- Kim JE, Cho HJ, Kim DD. Budesonide/cyclodextrin complex-loaded lyophilized microparticles for intranasal application. *Drug Dev Ind Pharm*. 2014;40(6):743–748.
- Constantin M, Bucatariu S, Harabagiu V, Ascenzi P, Fundueanu G. Do cyclodextrins bound to dextran microspheres act as sustained delivery systems of drugs? *Int J Pharm*. 2014;469(1):1–9.
- Khodaghali F, Eftekharzadeh B, Maghsoudi N, Rezaei PF. Chitosan prevents oxidative stress-induced amyloid  $\beta$  formation and cytotoxicity in NT2 neurons: involvement of transcription factors Nrf2 and NF- $\kappa$ B. *Mol Cell Biochem*. 2010;337(1–2):39–51.
- Arai K, Kinumaki T, Fujita T. Toxicity of chitosan. *Bull Tokai Reg Fish Lab*. 1968;43:89–94.
- Elnaggar YS, Etman SM, Abdelmonsif DA, Abdallah OY. Intranasal piperine-loaded chitosan nanoparticles as brain-targeted therapy in alzheimer's disease: optimization, biological efficacy, and potential toxicity. *J Pharm Sci*. 2015;104(10):3544–3556.
- Hwang SM, Chen CY, Chen SS, Chen JC. Chitinous materials inhibit nitric oxide production by activated RAW264.7 macrophages. *Biochem Biophys Res Commun*. 2000;271(1):229–233.
- Moosmann B, Behl C. Antioxidants as treatment for neurodegenerative disorders. *Expert Opin Investig Drugs*. 2002;11(10):1407–1435.
- Xie W, Xu P, Liu Q. Antioxidant activity of water-soluble chitosan derivatives. *Bioorg Med Chem Lett*. 2001;11(13):1699–1701.
- Zhang J, Tang Q, Xu X, Li N. Development and evaluation of a novel phytosome-loaded chitosan microsphere system for curcumin delivery. *Int J Pharm*. 2013;448(1):168–174.
- Morris R. Development of a water-maze procedure for studying spatial learning in the rat. *J Neurosci Methods*. 1984;11(1):47–60.
- Brandeis R, Brandys Y, Yehuda S. The use of the Morris Water Maze in the study of memory and learning. *Int J Neurosci*. 1989;48(1–2):29–69.
- Wu MN, Zhou LW, Wang ZJ, et al. Colivelin ameliorates amyloid  $\beta$  peptide-induced impairments in spatial memory, synaptic plasticity, and calcium homeostasis in rats. *Hippocampus*. 2015;25(3):363–372.
- He P, Davis SS, Illum L. Chitosan microspheres prepared by spray drying. *Int J Pharm*. 1999;187(1):53–65.
- Sander C, Madsen KD, Hyrup B, Nielsen HM, Rantanen J, Jacobsen J. Characterization of spray dried bioadhesive metformin microparticles for oromucosal administration. *Eur J Pharm Biopharm*. 2013;85(3 Pt A):682–688.
- Jensen DM, Cun D, Maltesen MJ, Frokjaer S, Nielsen HM, Foged C. Spray drying of siRNA-containing PLGA nanoparticles intended for inhalation. *J Control Release*. 2010;142(1):138–145.
- Chew NY, Chan HK. Use of solid corrugated particles to enhance powder aerosol performance. *Pharm Res*. 2001;18(11):1570–1577.
- Martín MJ, Calpena AC, Fernández F, Mallandrich M, Gálvez P, Clares B. Development of alginate microspheres as nystatin carriers for oral mucosa drug delivery. *Carbohydr Polym*. 2015;117:140–149.
- Zhang WF, Chen XG, Li PW, Liu CS, He QZ. Preparation and characterization of carboxymethyl chitosan and  $\beta$ -cyclodextrin microspheres by spray drying. *Drying Technol*. 2008;26(1):108–115.
- Wasnik S, Parmar P, Singh D, Ram A. Preparation and characterization of floating drug delivery system of azithromycin. *Acta Pol Pharm*. 2012;69(3):515–522.
- El-Sherbiny IM, Smyth HD. Controlled release pulmonary administration of curcumin using swellable biocompatible microparticles. *Mol Pharm*. 2012;9(2):269–280.
- Zhang WF, Chen XG, Li PW, He QZ, Zhou HY. Preparation and characterization of theophylline loaded chitosan/ $\beta$ -cyclodextrin microspheres. *J Mater Sci Mater Med*. 2008;19(1):305–310.
- Xu F, Yin M, Wu Y, Ding H, Song F, Wang J. Effects of drying methods on the preparation of dexamethasone-loaded chitosan microspheres. *Biomed Mater*. 2014;9(5):055003.
- Devrim B, Bozkır A, Canefe K. Preparation and evaluation of poly(lactic-co-glycolic acid) microparticles as a carrier for pulmonary delivery of recombinant human interleukin-2: II. In vitro studies on aerodynamic properties of dry powder inhaler formulations. *Drug Dev Ind Pharm*. 2011;37(11):1376–1386.
- Sinsuebpol C, Chatchawalsaisin J, Kulvanich P. Preparation and in vivo absorption evaluation of spray dried powders containing salmon calcitonin loaded chitosan nanoparticles for pulmonary delivery. *Drug Des Dev Ther*. 2013;7:861–873.
- Feng ZQ, Sun CG, Zheng ZJ, Hu ZB, Mu DZ, Zhang WF. Optimization of spray-drying conditions and pharmacodynamics study of theophylline/chitosan/ $\beta$ -cyclodextrin microspheres. *Drying Technol*. 2015;33:55–65.
- Iyer RM, Augsburger LL, Pope DG, Shah RD. Extrusion/spheronization-effect of moisture content and spheronization time on pellet characteristics. *Pharm Dev Technol*. 1996;1(4):325–331.
- Lazcano Z, Solis O, Bringas ME, et al. Unilateral injection of A $\beta$ 25-35 in the hippocampus reduces the number of dendritic spines in hyperglycemic rats. *Synapse*. 2014;68(12):585–594.
- Delobette S, Privat A, Maurice T. In vitro aggregation facilitates  $\beta$ -amyloid peptide – 25–35-induced amnesia in the rat. *Eur J Pharmacol*. 1997;319(1):1–4.
- D'Agostino G, Russo R, Avagliano C, Cristiano C, Meli R, Calignano A. Palmitoylethanolamide protects against the amyloid- $\beta$ 25-35-induced learning and memory impairment in mice, an experimental model of Alzheimer disease. *Neuropsychopharmacology*. 2012;37(7):1784–1792.
- Liu YM, Li ZY, Hu H, et al. Tenuifolin, a secondary saponin from hydrolysates of polygalasaponins, counteracts the neurotoxicity induced by A $\beta$ 25-35 peptides in vitro and in vivo. *Pharmacol Biochem Behav*. 2015;128:14–22.
- Schrott LM, Jackson K, Yi P, et al. Acute oral bryostatin-1 administration improves learning deficits in the APP/PS1 transgenic mouse model of Alzheimer's disease. *Curr Alzheimer Res*. 2015;12(1):22–31.
- Conde JR, Streit WJ. Microglia in the aging brain. *J Neuropathol Exp Neurol*. 2006;65(3):199–203.
- Mittal G, Carswell H, Brett R, Currie S, Kumar MN. Development and evaluation of polymer nanoparticles for oral delivery of estradiol to rat brain in a model of Alzheimer's pathology. *J Control Release*. 2011;150(2):220–228.
- Wegiel J, Imaki H, Wang KC, et al. Origin and turnover of microglial cells in fibrillar plaques of APPsw transgenic mice. *Acta Neuropathol*. 2003;105(4):393–402.
- Xue QS, Streit WJ. Microglial pathology in Down syndrome. *Acta Neuropathol*. 2011;122(4):455–466.

### Drug Design, Development and Therapy

Dovepress

### Publish your work in this journal

Drug Design, Development and Therapy is an international, peer-reviewed open-access journal that spans the spectrum of drug design and development through to clinical applications. Clinical outcomes, patient safety, and programs for the development and effective, safe, and sustained use of medicines are a feature of the journal, which

has also been accepted for indexing on PubMed Central. The manuscript management system is completely online and includes a very quick and fair peer-review system, which is all easy to use. Visit <http://www.dovepress.com/testimonials.php> to read real quotes from published authors.

Submit your manuscript here: <http://www.dovepress.com/drug-design-development-and-therapy-journal>